

Phase transition dynamics in the three-dimensional field-free $\pm J$ Ising model

Ozan S. Sariyer*

Piri Reis University, School of Arts and Sciences, Istanbul 34940 Turkey

(Dated: February 26, 2022)

By using frustration-preserving hard-spin mean-field theory, we investigated the phase transition dynamics in the three-dimensional field-free $\pm J$ Ising spin glass model. As the temperature T is decreased from paramagnetic phase at high temperatures, with a rate $\omega = -dT/dt$ in time t , the critical temperature depends on the cooling rate through a clear power-law ω^a . With increasing antiferromagnetic bond fraction p , the exponent a increases for the transition into the ferromagnetic case for $p < p_c$, and decreases for the transition into the spin glass phase for $p > p_c$, signaling the ferromagnetic-spin glass phase transition at $p_c \approx 0.22$. The relaxation time is also investigated, at adiabatic case $\omega = 0$, and it is found that the dynamic exponent $z\nu$ increases with increasing p .

I. INTRODUCTION

Spin glass systems exhibit aging, rejuvenation and memory effects owing to their long relaxation times.¹ Better understanding of the spin dynamics in such systems is a key for applications such as information storage, magnetic resonance imaging, biomarking, biosensing, and targeted drug delivery such as hyperthermia in cancer treatment.² Materials such as Fe_2TiO_5 , YEr (2%) and $\text{Fe}_{0.5}\text{Mn}_{0.5}\text{TiO}_3$ are classified as *Ising spin glasses*.³

In this paper, we study the dynamic effects on phase transitions in the $\pm J$ random-bond Ising spin glass model in zero external magnetic field that is defined on a lattice by the dimensionless Hamiltonian⁴

$$\mathcal{H} = - \sum_{\langle ij \rangle} J_{ij} s_i s_j. \quad (1)$$

Here, the sum is over ij -bonds, $s_i = \{+1, -1\}$ is the Ising spin at i -site, and $J_{ij} = \{+J, -J\}$ is the ij -bond interaction dealt quench-randomly, with an antiferromagnetic ($-J$) probability p . A dimensionless temperature for the system can be defined as $T = 1/J$.

The hard-spin mean-field theory (HSMFT) is defined by the set of self-consistent equations

$$m_i = \sum_{\{s_j\}} \left\{ \left[\prod_j \frac{1 + m_j s_j}{2} \right] \tanh \left(\sum_j J_{ij} s_j \right) \right\} \quad (2)$$

for the local magnetization m_i at each i -site, with nearest-neighbors labeled by j . For it preserves the local frustration, it is useful in studying spin glass systems.⁵⁻²⁴

Previously, we studied the $\pm J$ model on a simple cubic lattice under time-dependent external magnetic field by HSMFT, and obtained the phase diagram (see Fig. 1) from distinctive behavior of hysteresis loops.²⁴ At temperatures above a critical T_c^0 that depends on p , system is in paramagnetic (PM) phase. (In general, the critical temperature $T_c(\omega)$ depends on the cooling rate ω , and $T_c^0 \equiv T_c(\omega = 0)$ denotes the non-dynamic critical temperature at infinitely-slow cooling rate.) At low temperatures, $T < T_c^0(p)$, there exist a ferromagnetic (FM) phase for $p < p_c$, and a spin glass (SG) phase for $p > p_c$. The

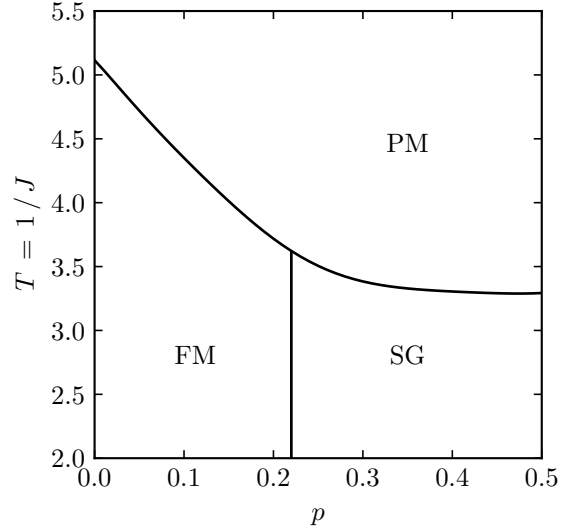


FIG. 1. Zero-field phase diagram of the $\pm J$ model on a simple cubic lattice. PM, FM, and SG respectively denote paramagnetic, ferromagnetic, and spin glass phases.

FM-SG phase boundary is at $p_c \approx 0.22$. The phase diagram of Fig. 1 is consistent both with theoretical²⁵ and experimental²⁶ results, and is mirror symmetric about $p = 0.5$, with antiferromagnetic (AFM) phase replacing the FM phase for $p > 1 - p_c$. We can omit the $p > 0.5$ subspace in general, due to the FM \leftrightarrow AFM symmetry of classical Ising spins on bipartite lattices.

In the same previous work, dynamic effect of the magnetic field sweep rate on the dissipative loss in a hysteresis cycle was also studied²⁴, while in the present article, we consider the dynamics of the model by means of (i) adiabatic relaxation time behavior for infinitely-slow cooling rate $\omega = 0$, and (ii) the effects of nonzero cooling rate ω on the critical temperature $T_c(\omega)$.

To this end, we consider an $L \times L \times L$ -site simple cubic lattice with periodic boundary conditions. HSMFT results become independent of the lattice size for $L > 15$ for this system^{20,24}, and we work with $L = 20$ here.

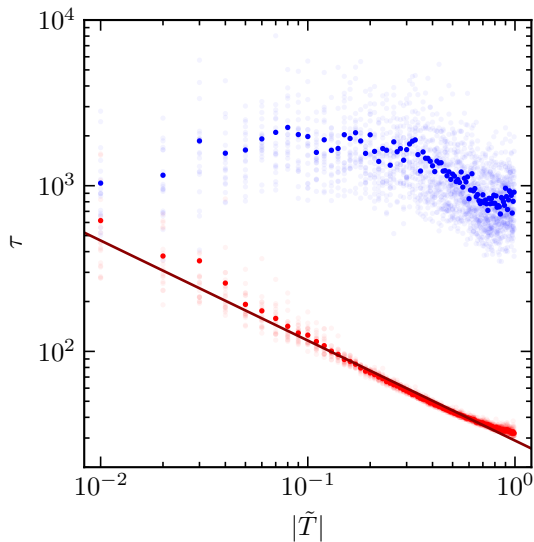


FIG. 2. Relaxation time τ as a function of absolute reduced temperature $|\tilde{T}| = |T - T_c^0|/T_c^0$ for $p = 0.25$. Faded markers show the results for 20 distinct realizations of AFM bond distributions, while the dark markers show averages over those random replicas. Blue and red show the data below and above the critical temperature, $\tilde{T} < 0$ and $\tilde{T} > 0$ respectively. Line is the best fit to the power-law Eq. (4), for $\tilde{T} \geq 0.1$.

II. RELAXATION TIME

A particular realization at a given (T, p) is generated by the assignment of the quenched-random interactions $J_{ij} = \pm 1/T$ with a probability p of AFM bonds $-1/T$, and initially, an unbiased random assignment of spins in the range $s_i \in [-1, +1]$. A time step dt corresponds to successive iterations of Eq. (2) on L^3 randomly chosen sites. The relaxation time τ corresponds to number of such time steps required for the system to converge from an initial random seed to a self-consistent solution that is determined when the mean-square deviation in magnetization, $\Delta m^2 = L^{-3} \sum_i [m_i(\tau) - m_i(\tau - 1)]^2$, drops below a predetermined threshold, *i.e.*, when $\Delta m^2 \leq 10^{-12}$.

A characteristic signature of spin glass systems is that the relaxation time τ diverges as $T \rightarrow T_c^{0+}$, and remains infinite for $T < T_c^0$. Fig. 2 is a log-log plot of the relaxation time τ as a function of $|\tilde{T}|$, for a representative value $p = 0.25$, while we obtain the same behavior for other p values. Here,

$$\tilde{T} \equiv \frac{T - T_c^0}{T_c^0} \quad (3)$$

is the reduced temperature that measures the distantness to critical temperature. Faded markers show the results for 20 distinct realizations of AFM bond distributions, while the dark markers show averages over such random realizations. We see that the relaxation time τ averaged over replicas, peaks as $\tilde{T} \rightarrow 0^+$ and stays at large values for $\tilde{T} < 0$ as expected. Deviation from a true divergence at $\tilde{T} \leq 0$ is due to finite-size effects.

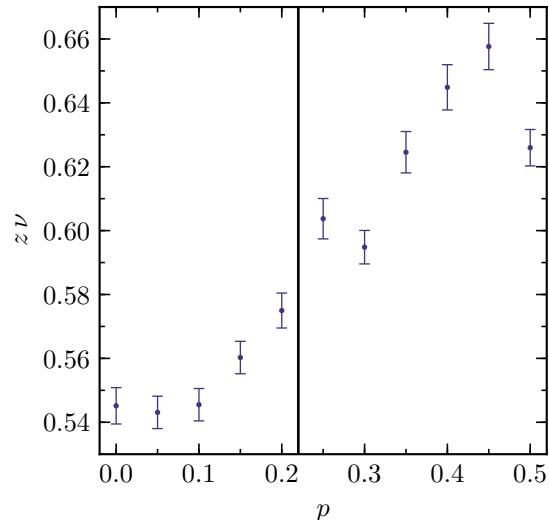


FIG. 3. Dynamic critical exponent $z\nu$ as a function of AFM bond fraction p . Error bars show the standard deviation of the fit procedure to Eq. (4). Vertical line shows the critical $p_c \approx 0.22$ between the ordered FM and SG phases (see Fig. 1).

The divergence of τ as $\tilde{T} \rightarrow 0^+$, referred as the critical slowing-down, is due to the divergence of the correlation length ξ . A scaling relation between the relaxation time and the correlation length $\tau \sim \xi^z$, and another one between the correlation length and the reduced temperature, $\xi \sim \tilde{T}^{-\nu}$, yield to the power-law²⁶

$$\tau \sim \tilde{T}^{-z\nu}. \quad (4)$$

Fitting the average relaxation time to Eq. (4) in the range $0.1 \leq \tilde{T} \leq 1$, we obtain the line in Fig. 2. Following the same procedure for several p values, we obtain the dynamic critical exponent $z\nu$ as a function of AFM bond concentration p , as presented in Fig. 3. We observe that $z\nu$ increases with increasing p .

III. FINITE TEMPERATURE SWEEP RATE

To determine the effect of finite cooling rate

$$\omega = -\frac{dT}{dt} \neq 0 \quad (5)$$

on the critical temperature $T_c(\omega)$, we start with a fully relaxed realization of the system at a fixed AFM bond distribution at a high temperature, $T = 100$. The system is then cooled with a rate of change in temperature $-dT$ per time step. As defined above, one time step dt corresponds to updating L^3 randomly chosen sites according to Eq. (2). We repeat the procedure for ω spanning two orders of magnitude in the range $[0.00025, 0.025]$, and for various p . For each set of values for ω and p , we generate 20 distinct realizations of AFM bond distributions and work with the averages over those replicas.

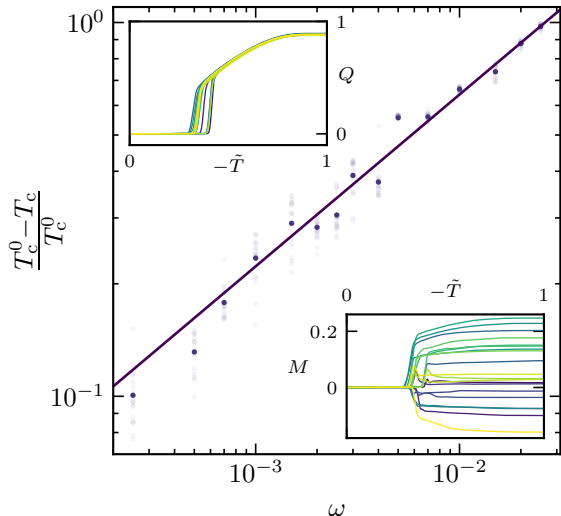


FIG. 4. Reduced difference $(T_c^0 - T_c)/T_c^0$ between the apparent dynamic (T_c) and the true non-dynamic (T_c^0) critical temperatures, as a function of cooling rate ω , for $p = 0.25$. Faded markers show the results for 20 distinct realizations of AFM bond distributions, while the dark markers show averages over those random replicas. The line shows the best fit to the power-law Eq. (6). The average magnetization, $M = L^{-3} \sum_i m_i$ and the SG order parameter $Q = L^{-3} \sum_i m_i^2$ are shown in the bottom-right and top-left insets as functions of $-\tilde{T}$ for all 20 realizations for $\omega = 0.0025$.

For finite $\omega \neq 0$, the system will not find enough time to fully relax to an ordered state when it reaches at the true non-dynamic critical temperature $T_c^0 = T_c(\omega = 0)$. And when it reaches an ordered state, the temperature will be already cooled below T_c^0 . Thus, the apparent critical temperature $T_c(\omega)$ is expected to be lower than T_c^0 , and to shift down with increasing cooling rate ω .

The reduced difference $(T_c^0 - T_c)/T_c^0$ between the apparent dynamic T_c and the true non-dynamic T_c^0 is plotted in Fig. 4 in log-log axes as a function of ω , for a representative value $p = 0.25$, while we obtain the same behavior for other p values. The average magnetization, $M = L^{-3} \sum_i m_i$ (shown in the bottom-right inset for 20 distinct realizations for $p = 0.25$ and $\omega = 0.0025$), is not suitable to determine T_c for PM-SG phase transition at $p > p_c$. Instead, the SG order parameter $Q = L^{-3} \sum_i m_i^2$ (shown in the top-left inset for 20 distinct realizations for $p = 0.25$ and $\omega = 0.0025$) is used for the whole range of p , implementing the fact that $Q = 0$ for $T > T_c$ and $Q > 0$ for $T < T_c$. We checked that for $\omega = 0$, this condition yields the same equilibrium PM phase boundary as obtained from hysteretic behavior (see Fig. 1).

Particularly at higher ω , the reduced difference in critical temperatures shows a clear power-law behavior,

$$\frac{T_c^0 - T_c}{T_c^0} \sim \omega^a, \quad (6)$$

as shown by the fit of average data to Eq. (6), resulting in the line in Fig. 4. Such is the case for all other p

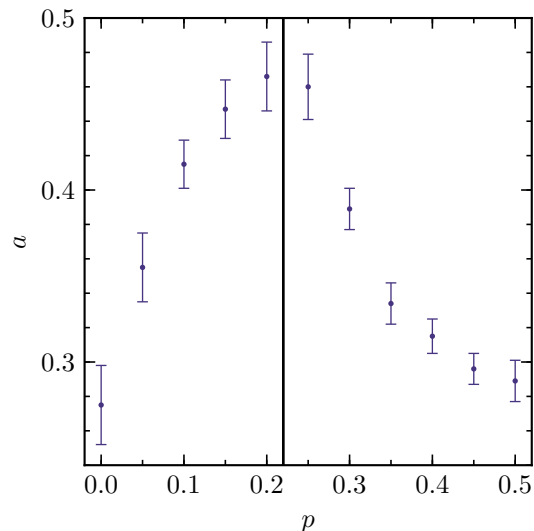


FIG. 5. Temperature sweep rate exponent a of Eq. (6) as a function of AFM bond fraction p . Error bars show the standard deviation of the fit procedure to Eq. (6). Vertical line shows the critical $p_c \approx 0.22$ between the ordered FM and SG phases (see Fig. 1).

values, and the resulting exponents are shown in Fig. 5 for various p . We clearly observe the peak in the exponent a at the FM-SG phase transition at $p_c \approx 0.22$.

IV. CONCLUSION

We simulated the phase transition dynamics of $\pm J$ Ising spin glass model on a simple cubic lattice by the frustration preserving hard-spin mean-field theory. We obtained the dynamic exponents $z\nu$ for the relaxation time, and a for the cooling rate dependence of critical temperature, $T_c(\omega)$.

We found that the dynamic exponent $z\nu$ varies in the range of about 0.5 to 0.7, which is an order of magnitude smaller than the values reported by AC magnetometry experiments^{2,3,27-34} and stochastic simulations^{35,36}. Such is the pitfall of mean-field theories in general. Neglecting the long range correlations close to critical points where correlation length diverges, mean-field theories exhibit inadequate values for critical temperatures, amplitudes and exponents. However, they offer qualitative pictures of phase transitions. In this particular case, although our values for the dynamic exponent $z\nu$ do not agree with previous results, the qualitative feature that it increases with increasing AFM bond ratio p is acceptable. This can be understood on the basis of increasing relaxation time with increasing frustration (increasing raggedness and number of local minima in the free energy landscape) with increasing p . This may also explain the various experimental values for $z\nu$ ranging in the range from 5.6 ± 0.1 for $\text{Sn}_{0.9}\text{Fe}_{3.1}\text{N}^{34}$ to 10.4 ± 1.0 for $\text{Fe}_{0.5}\text{Mn}_{0.5}\text{TiO}_3$ ²⁷.

Similarly, although the values might be incorrect, the cooling rate exponent a shows a peak at $p = p_c \approx 0.22$, which clearly indicates the FM-SG transition. In these simulations, we initialized the cooling from a high temperature $T = 100$. We observed that starting the cooling from $T = 10$, changes our results only within the standard deviations even for the highest cooling rates, and hence, we infer that $T = 100$ is a safe high-temperature starting point. Nonetheless, the effect of initial temperature on the dynamic properties, is another interesting direction to cover. We expect that as the starting temperature gets smaller, the apparent dynamic critical temper-

atures will decrease further. This is because the system will find even smaller times to relax to an ordered state, and by the time it relaxes, the temperature will be even more smaller than the true non-dynamic T_c^0 .

ACKNOWLEDGMENTS

I thank Dr. Aykut Erbaş for valuable discussions and for careful reading of the manuscript. Numerical calculations were run by a machine partially supported by the 2232 TÜBİTAK Reintegration Grant of project #115C135.

-
- * ossariyer@pirireis.edu.tr
- ¹ V. Dupuis, E. Vincent, J.-P. Bouchaud, J. Hammann, A. Ito, and H. A. Katori, *Phys. Rev. B* **64**, 174204 (2001).
 - ² M. Perovic, V. Kusigerski, V. Spasojevic, A. Mrakovic, J. Blanus, M. Zentkova, and M. Mihalik, *J. Phys. D* **46**, 165001 (2013).
 - ³ P. Svedlindh, K. Gunnarsson, P. Nordblad, L. Lundgren, A. Ito, and H. Aruga, *J. Magn. Magn. Mater.* **71**, 22 (1987).
 - ⁴ G. Toulouse, *Communications on Physics* **2**, 115 (1977).
 - ⁵ J. R. Banavar, M. Cieplak, and A. Maritan, *Phys. Rev. Lett.* **67**, 1807 (1991).
 - ⁶ R. R. Netz and A. N. Berker, *Phys. Rev. Lett.* **66**, 377 (1991).
 - ⁷ R. R. Netz and A. N. Berker, *Phys. Rev. Lett.* **67**, 1808 (1991).
 - ⁸ R. R. Netz and A. N. Berker, *J. Appl. Phys.* **70**, 6074 (1991).
 - ⁹ R. Netz, *Phys. Rev. B* **46**, 1209 (1992).
 - ¹⁰ R. Netz, *Phys. Rev. B* **48**, 16113 (1993).
 - ¹¹ E. A. Ames and S. R. McKay, *J. Appl. Phys.* **76**, 6197 (1994).
 - ¹² A. Berker, A. Kabakçioğlu, R. Netz, and M. Yalabık, *Turk. J. Phys.* **18**, 354 (1994).
 - ¹³ A. Kabakçioğlu, A. N. Berker, and M. C. Yalabık, *Phys. Rev. E* **49**, 2680 (1994).
 - ¹⁴ G. B. Akgüç and M. C. Yalabık, *Phys. Rev. E* **51**, 2636 (1995).
 - ¹⁵ J. E. Tesiero and S. R. McKay, *J. Appl. Phys.* **79**, 6146 (1996).
 - ¹⁶ J. L. Monroe, *Phys. Lett. A* **230**, 111 (1997).
 - ¹⁷ A. Pelizzola and M. Pretti, *Phys. Rev. B* **60**, 10134 (1999).
 - ¹⁸ A. Kabakçioğlu, *Phys. Rev. E* **61**, 3366 (2000).
 - ¹⁹ H. Kaya and A. N. Berker, *Phys. Rev. E* **62**, R1469 (2000).
 - ²⁰ B. Yücesoy and A. N. Berker, *Phys. Rev. B* **76**, 014417 (2007).
 - ²¹ M. D. Robinson, D. P. Feldman, and S. R. McKay, *Chaos* **21**, 037114 (2011).
 - ²² T. Çağlar and A. N. Berker, *Phys. Rev. E* **84**, 051129 (2011).
 - ²³ T. Çağlar and A. N. Berker, *Phys. Rev. E* **92**, 062131 (2015).
 - ²⁴ O. S. Sariyer, A. Kabakçioğlu, and A. N. Berker, *Phys. Rev. E* **86**, 041107 (2012).
 - ²⁵ Y. Ozeki and H. Nishimori, *J. Phys. Soc. Jpn.* **56**, 1568 (1987).
 - ²⁶ K. Binder and A. P. Young, *Rev. Mod. Phys.* **58**, 801 (1986).
 - ²⁷ P. Svedlindh, P. Granberg, P. Nordblad, L. Lundgren, and H. S. Chen, *Phys. Rev. B* **35**, 268 (1987).
 - ²⁸ A. Mauger, J. Ferré, M. Ayadi, and P. Nordblad, *Phys. Rev. B* **37**, 9002 (1988).
 - ²⁹ K. Gunnarsson, P. Svedlindh, P. Nordblad, L. Lundgren, H. Aruga, and A. Ito, *Phys. Rev. Lett.* **61**, 754 (1988).
 - ³⁰ D. N. H. Nam, R. Mathieu, P. Nordblad, N. V. Khiem, and N. X. Phuc, *Phys. Rev. B* **62**, 8989 (2000).
 - ³¹ J. A. Quilliam, S. Meng, C. G. A. Mugford, and J. B. Kycia, *Phys. Rev. Lett.* **101**, 187204 (2008).
 - ³² B. S. Wang, P. Tong, Y. P. Sun, X. B. Zhu, Z. R. Yang, W. H. Song, and J. M. Dai, *Appl. Phys. Lett.* **97**, 042508 (2010).
 - ³³ M. Perovic, A. Mrakovic, V. Kusigerski, J. Blanus, and V. Spasojevic, *J. Nanopart. Res.* **13**, 6805 (2011).
 - ³⁴ T. Scholz and R. Dronskowski, *AIP Adv.* **6**, 055107 (2016).
 - ³⁵ A. T. Ogielski and I. Morgenstern, *Phys. Rev. Lett.* **54**, 928 (1985).
 - ³⁶ A. T. Ogielski, *Phys. Rev. B* **32**, 7384 (1985).